

Slow growth of *Mycobacterium tuberculosis* at acidic pH is regulated by *phoPR* and host-associated carbon sources

Jacob J. Baker, Benjamin K. Johnson and
Robert B. Abramovitch*
Department of Microbiology and Molecular Genetics,
Michigan State University, East Lansing, MI 48824,
USA.

Summary

During pathogenesis, *Mycobacterium tuberculosis* (Mtb) colonizes environments, such as the macrophage or necrotic granuloma, that are acidic and rich in cholesterol and fatty acids. The goal of this study was to examine how acidic pH and available carbon sources interact to regulate Mtb physiology. Here we report that Mtb growth at acidic pH requires host-associated carbon sources that function at the intersection of glycolysis and the TCA cycle, such as pyruvate, acetate, oxaloacetate and cholesterol. In contrast, in other tested carbon sources, Mtb fully arrests its growth at acidic pH and establishes a state of non-replicating persistence. Growth-arrested Mtb is resuscitated by the addition of pyruvate suggesting that growth arrest is due to a pH-dependent checkpoint on metabolism. Additionally, we demonstrate that the *phoPR* two-component regulatory system is required to slow Mtb growth at acidic pH and functions to maintain redox homeostasis. Transcriptional profiling and functional metabolic studies demonstrate that signals from acidic pH and carbon source are integrated to remodel pathways associated with anaplerotic central metabolism, lipid anabolism and the regeneration of oxidized cofactors. Because *phoPR* is required for Mtb virulence in animals, we suggest that pH-driven adaptation may be critical to Mtb pathogenesis.

Introduction

Mycobacterium tuberculosis (Mtb) is a slow growing bacterial pathogen. During growth *in vitro*, in macrophages, or in mice, Mtb has measured doubling times ranging from ~20 h to 70 days (Muñoz-Elias *et al.*, 2005; Gill *et al.*, 2009; Rohde *et al.*, 2012). Under low oxygen, Mtb enters

Accepted 21 June, 2014. *For correspondence. E-mail abramov5@msu.edu; Tel. (+1) 517 884 5416; Fax (+1) 517 353 8957.

a non-replicating persistent (NRP) state where the pathogen arrests growth but remains viable. Slow or arrested growth is thought to play an important role in the establishment of chronic infections and drug resistance. Understanding how Mtb regulates its growth rate in response to environmental cues encountered during infection, including acidic pH and carbon source availability, should provide insight into the physiology that makes Mtb a successful and difficult to treat pathogen.

Mtb growth and gene expression are strongly regulated by environmental pH (Piddington *et al.*, 2000; Vandal *et al.*, 2008; 2009a,b; Abramovitch *et al.*, 2011). In rich medium, the bacterium slows its growth below pH 6.4 and arrests its growth at ~pH 5.0 (Abramovitch *et al.*, 2011). Following 1 day of exposure to an acidic environment at pH 4.5, Mtb maintains an intracellular pH of ~7.4, demonstrating that Mtb effectively buffers its cytoplasm and that changes in growth rate are not solely associated with cytoplasmic acidification (Vandal *et al.*, 2008). Mutation of the Rv3671c membrane protein causes a loss of cytoplasmic pH-homeostasis and results in strong attenuation of virulence during mouse infection, supporting the idea that Mtb encounters environments *in vivo* where acidic pH-dependent adaptations are essential for pathogenesis (Vandal *et al.*, 2008).

Transcriptional profiling studies of Mtb in response to acidic pH *in vitro* and in macrophages demonstrate widespread changes in gene expression (Fisher *et al.*, 2002; Rohde *et al.*, 2007). The phagosomal acidic pH regulon (Rohde *et al.*, 2007) exhibits significant overlap with the *phoPR* two-component regulatory system (TCS) regulon (Walters *et al.*, 2006; Gonzalo-Asensio *et al.*, 2008), suggesting that *phoPR* may play a role in pH-driven adaptation. For example, the acid and phagosome regulated locus, *aprABC*, is strongly induced by acidic pH, requires *phoP* for its expression, and its promoter is strongly bound by the PhoP response regulator (Abramovitch *et al.*, 2011; Galagan *et al.*, 2013). *phoPR* mutants are highly attenuated during mouse and guinea pig infections (Perez *et al.*, 2001; Martin *et al.*, 2006), further supporting that pH-driven adaptation plays an important role during the course of infection.

Several PhoPR-regulated, acidic-pH induced genes are associated with carbon metabolism. For example, the *pks2*, *pks3*, and *pks4* genes are associated with the pro-

duction of cell envelope lipids sulpholipid, diacyl- and polyacyltrehalose (DAT and PAT) (Asensio *et al.*, 2006; Walters *et al.*, 2006), and the *aprABC* locus is associated with the control of triacylglycerol (TAG) accumulation and regulation of genes of central carbon and propionate metabolism (Abramovitch *et al.*, 2011). While all the carbon sources available to *Mtb* *in vivo* are not specifically known, the requirement for isocitrate lyase (*icl*) during infection suggests that *Mtb* is metabolizing acetyl-CoA derived from long chain fatty acids via the glyoxylate shunt (McKinney *et al.*, 2000), or propionyl-CoA derived from cholesterol via the methylcitrate cycle (Upton and McKinney, 2007; Savvi *et al.*, 2008; Eoh and Rhee, 2014). Several lines of evidence support that cholesterol is an important carbon source during infection. For example, in macrophages, *Mtb* metabolizes cholesterol, and likely other lipids available on low-density lipoprotein, as carbon sources (Pandey and Sassetti, 2008; Russell *et al.*, 2009); cholesterol and TAG are abundant lipids in the caseum of the human *Mtb* granuloma (Kim *et al.*, 2010); and, several genes involved in cholesterol catabolism are essential for *in vivo* survival (Pandey and Sassetti, 2008; Chang *et al.*, 2009). *Mtb* has also been shown to acquire and metabolize macrophage derived fatty acids (Lee *et al.*, 2013). The catabolism of cholesterol and fatty acids is predicted to produce acetyl-CoA, propionyl-CoA, pyruvate, and glycerol (Van der Geize *et al.*, 2007), suggesting *Mtb* physiology may be regulated by these host-associated carbon sources.

Both the macrophage phagosome and the caseum of a necrotic granuloma can be acidic environments (Dannenberg, 2006); therefore, it is possible that *Mtb* integrates environmental signals from acidic pH and carbon nutrient availability to modulate its growth and metabolism. Indeed, Baek and colleagues have shown that a TAG synthase mutant (*tgs1*) has enhanced growth at acidic pH as compared to the wild-type (WT) strain, genetically linking acidic pH, carbon metabolism, and growth rate (Baek *et al.*, 2011). In this study, we explore the hypothesis that acidic pH and available carbon sources interact to regulate *Mtb* growth and physiology.

Results

Mtb exhibits carbon source specific growth arrest at acidic pH

Mtb has been shown to slow its growth at acidic pH in a variety of rich and minimal media (Piddington *et al.*, 2000; Vandal *et al.*, 2008; Abramovitch *et al.*, 2011; Baek *et al.*, 2011). To confirm these observations, *Mtb* strain CDC1551 was grown in 7H9 (OADC) medium buffered at pH 7.0 or pH 5.7 using 100 mM MOPS or MES respectively. Following 9 days of incubation at pH 5.7, *Mtb* exhibited a fourfold reduction in growth relative to *Mtb* grown at pH 7.0 (Fig.

S1A). We hypothesized that changes in carbon metabolism may be associated with pH-dependent slowed growth. 7H9 (OADC) medium contains a variety of potential carbon sources including glycerol, glucose, oleic acid, albumin, amino acids and tween-80. In order to isolate the role of specific carbon sources, we investigated the growth of *Mtb* at pH 7.0 and 5.7 in a defined, buffered minimal medium (Lee *et al.*, 2013). We first tested glucose and glycerol as carbon sources and observed that *Mtb* fully arrests its growth at pH 5.7 in the presence of these carbon sources alone or combined (Fig. S1B and C). In glycerol-amended medium, *Mtb* begins to exhibit slowed growth at pH 6.4, consistent with previous observations in rich medium (Abramovitch *et al.*, 2011).

Given the observation of growth arrest in medium supplemented with glycolytic carbon sources, *Mtb* growth was examined in the presence of a variety of carbon sources associated with central metabolism (Fig. 1A, Fig. S2). For these experiments, *Mtb* cultures were grown in rich medium, pelleted and then seeded at an initial density of OD 0.05 in standing, vented flasks containing 8 ml of buffered minimal medium and a single carbon source. Cultures were incubated for 9 days and growth was measured at 3-day intervals. As a control, to determine the effect of residual extracellular or intracellular carbon sources, cultures were also seeded in medium without the addition of a carbon source. In this 'No Carbon' control, very little growth was observed at pH 7.0 and no growth was observed at pH 5.7 (Fig. 1A, Fig. S2), supporting that growth above this baseline is promoted by metabolism of the specified carbon source. For the carbon sources that supported growth at pH 7.0, it was observed that at pH 5.7, some carbon sources restricted growth while others permitted growth (Fig. 1A, Fig. S2). Notably, carbon sources that feed central metabolism at the intersection of glycolysis and the TCA cycle permitted growth at acidic pH, including: phosphoenolpyruvate (PEP), pyruvate, oxaloacetate, and acetate (Fig. 1A). Pyruvate was the preferred carbon source at pH 5.7, with similar growth relative to pH 7.0 (Fig. 1B). In a long-term 36-day growth experiment, *Mtb* cultured in 10 mM glycerol at pH 7.0 reaches stationary phase, while at pH 5.7 the culture remains growth-arrested, showing that the 9-day trends extend to stationary phase and that differing total biomasses are achieved. In contrast, cultures incubated in 10 mM pyruvate at acidic and neutral pH over 36 days reach a similar optical density at stationary phase (Fig. S3A). *Mtb* cholesterol catabolism is predicted to generate pyruvate, acetyl-CoA and propionyl-CoA and indeed, cholesterol also permitted modest growth at acidic pH (Fig. 1A, Fig. S2). Together, these data demonstrate that the ability of *Mtb* to grow at acidic pH is carbon source-specific. The growth permissive carbon sources all feed central metabolism at a switch point in metabolism known as the PEP-pyruvate-

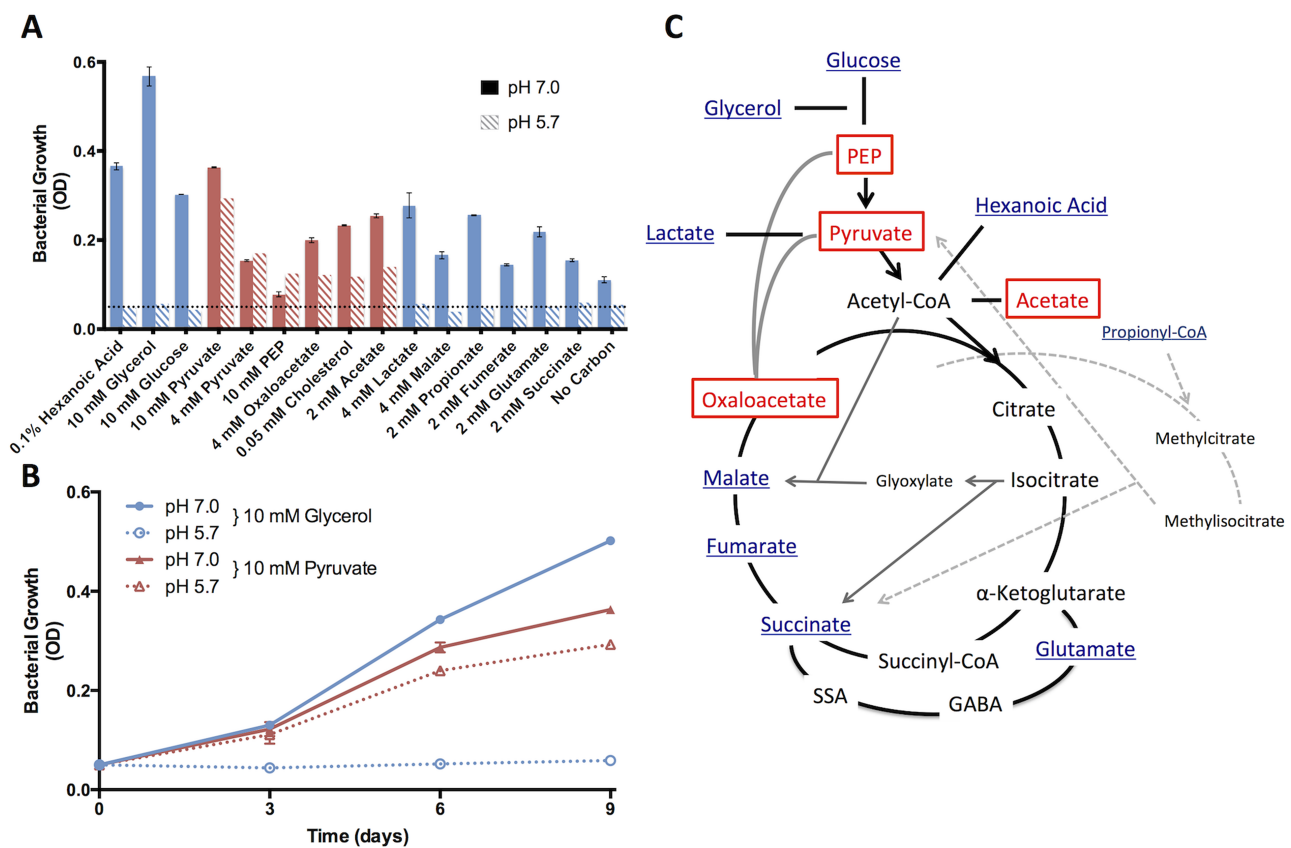


Fig. 1. Mtb exhibits carbon source-specific growth arrest at acidic pH.

A. Mtb growth on various carbon sources at both neutral and acidic pH. Cultures were seeded at a starting density of 0.05 OD₆₀₀ (horizontal dotted line) and growth was measured every 3 days for 9 days. The growth curves are presented in Fig. S2 and the day 9 end-point data are summarized in this panel. Carbon sources are designated as either permissive (red bars) or restrictive (blue bars) for growth at acidic pH, as compared to the growth baseline in the 'No Carbon' control. Only PEP, pyruvate, oxaloacetate, acetate and cholesterol promoted growth at acidic pH.

B. Growth curves showing glycerol arrests growth and pyruvate promotes growth of Mtb at acidic pH.

C. Model showing the position within central carbon metabolism of carbon sources permissive (boxed) and restricted (underlined) for growth at acidic pH. The panel is modified from Tian *et al.* (2005). Error bars represent the standard deviation and the data are representative of two independent experiments.

oxaloacetate node or anaplerotic node (Sauer and Eikmanns, 2005). Therefore, our findings suggest that metabolic flexibility afforded by carbon sources feeding the anaplerotic node may play a role in promoting growth in acidic environments (Fig. 1C).

pH-driven, carbon source-dependent growth arrest is species specific

During pathogenesis, Mtb will encounter environments with acidic pH and restricted carbon sources; therefore we hypothesized that the pH-dependent growth arrest phenotype may have evolved as a pathogenesis-specific adaptation. Previously, Piddington and colleagues observed that Mtb grown in pH 6.0 Sauton's medium (where glycerol is the primary carbon source) exhibits strongly restricted growth at acidic pH, as compared to a modest decrease in

growth with the non-pathogenic, environmental species *Mycobacterium smegmatis* (Piddington *et al.*, 2000). To determine if pH- and carbon source-specific growth arrest is an evolved pathogenesis trait, the growth of the non-pathogenic species *M. smegmatis* was examined in a variety of single carbon sources at acidic and neutral pH. In contrast to Mtb, the growth of *M. smegmatis* was not slowed at pH 5.7 in any of the tested carbon sources, except glycerol, where there was an ~30% reduction in growth (Fig. S4A). The lack of carbon source-specific growth arrest at acidic pH in *M. smegmatis* supports an evolutionary model whereby this physiology may function to promote pathogenesis in animals.

Given that differences exist in the physiology and virulence of different Mtb strains (Homolka *et al.*, 2010), we examined if the growth arrest phenotype observed in CDC1551 was conserved in other Mtb strains. The Mtb

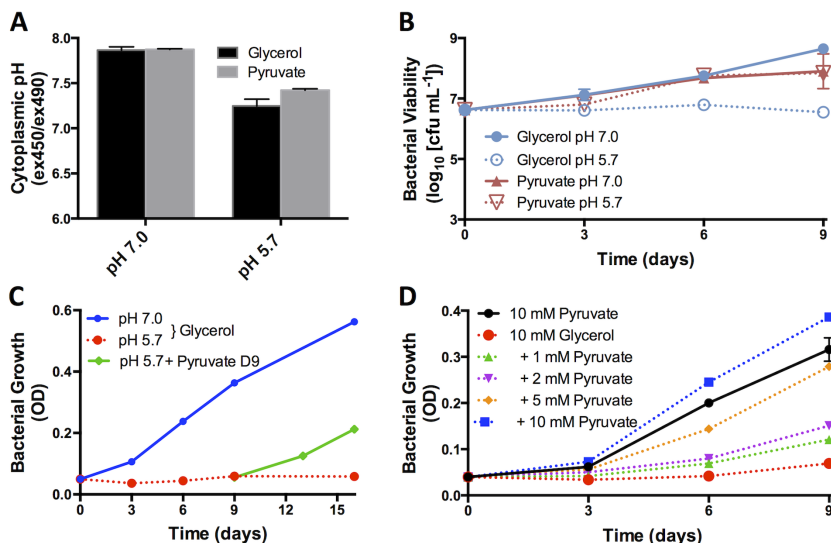


Fig. 2. Growth-arrested Mtb is resuscitated with pyruvate.

A. Mtb can maintain its cytoplasmic pH homeostasis in response to both glycerol and pyruvate at pH 7.0 and pH 5.7.

B. Mtb remains viable during acidic pH growth arrest as measured by colony-forming units (cfu). This finding suggests that Mtb enters a state of non-replicating persistence driven by acidic pH and carbon source.

C. Following 9 days of growth arrest in minimal medium with 10 mM glycerol at pH 5.7, addition of 10 mM pyruvate resuscitates Mtb growth (green line). Therefore, Mtb growth arrest at acidic pH is reversible and non-lethal.

D. Pyruvate promotes Mtb growth in 10 mM glycerol in a concentration-dependent manner. Error bars represent the standard deviation and the data are representative of three individual experiments.

strains CDC1551, H37Rv, HN878, and Erdman were all grown at pH 7.0 or pH 5.7 in the presence of either glycerol or pyruvate. Consistent with CDC1551, all of the strains grew well on glycerol at pH 7.0, but were arrested for growth at pH 5.7 (Fig. S4B). Pyruvate as a single carbon source allowed growth at both pH 7.0 and pH 5.7 for each strain, albeit with differences in the magnitude of growth (Fig. S4B). This finding supports that the carbon source-specific growth arrest observed in CDC1551 is qualitatively consistent with other Mtb strains.

Intracellular pH homeostasis and viability are maintained during growth arrest

To investigate the physiology of pH-dependent growth arrest, we examined the effect of growth arrest on intracellular pH homeostasis and viability. Previously, in rich medium at acidic pH, it has been shown that Mtb maintains intracellular pH homeostasis (Vandal *et al.*, 2008). However, it is possible that in minimal medium, Mtb is impaired in maintaining pH homeostasis. To determine if pH-dependent growth arrest was associated with a loss of pH-homeostasis, intracellular pH was quantified using an assay employing the pH-sensitive fluorescent dye CMFDA (Purdy *et al.*, 2009). Mtb grown in minimal medium with glycerol or pyruvate at pH 5.7 exhibited a slight acidification of the cytoplasm as compared to growth at pH 7.0 (Fig. 2A). However, at pH 5.7, there was no significant difference between the cytoplasmic pH of Mtb under growth restrictive or permissive conditions. Therefore, Mtb is capable of maintaining pH homeostasis at pH 5.7 in both glycerol and pyruvate, and intracellular pH is not associated with differential growth.

To determine if growth-arrested cells were viable, colony-forming units (cfu) were counted for Mtb grown in

minimal medium, at pH 7.0 or 5.7, with glycerol or pyruvate as a sole carbon source. No significant reduction in bacterial viability was observed in Mtb cultured at pH 5.7 with glycerol over the 9-day time-course, showing that growth-arrested Mtb maintains its viability in the absence of growth (Fig. 2B). Thus, growth arrest is not due to glycerol-mediated toxicity and cell death.

Pyruvate resuscitates growth-arrested Mtb

The viability of growth-arrested Mtb raised the possibility that the bacteria may be resuscitated with a growth permissive carbon source. To test this hypothesis, following 9 days of growth arrest on glycerol at pH 5.7, 10 mM pyruvate was added to the culture. Remarkably, pyruvate resuscitated growth-arrested Mtb (Fig. 2C), even in the continued presence of 10 mM glycerol in the medium, demonstrating bacterial viability and the growth permissive effect of pyruvate is dominant over the growth restrictive effect of glycerol.

To further explore the growth permissive activity of pyruvate, Mtb growth in 10 mM glycerol at pH 5.7 was examined with increasing amounts of pyruvate (from 1 mM to 10 mM). At pH 5.7, pyruvate relieved glycerol-dependent growth arrest in a concentration-dependent manner (Fig. 2D). Mtb grown with 10 mM of both pyruvate and glycerol, showed improved growth as compared to 10 mM pyruvate alone, suggesting the addition of pyruvate enables the co-metabolism of glycerol. Together, these findings demonstrate that Mtb integrates environmental pH and available carbon source to control its growth. Indeed, Mtb appears to establish a state of NRP under acidic pH with glycerol and can be resuscitated in the presence of pyruvate.

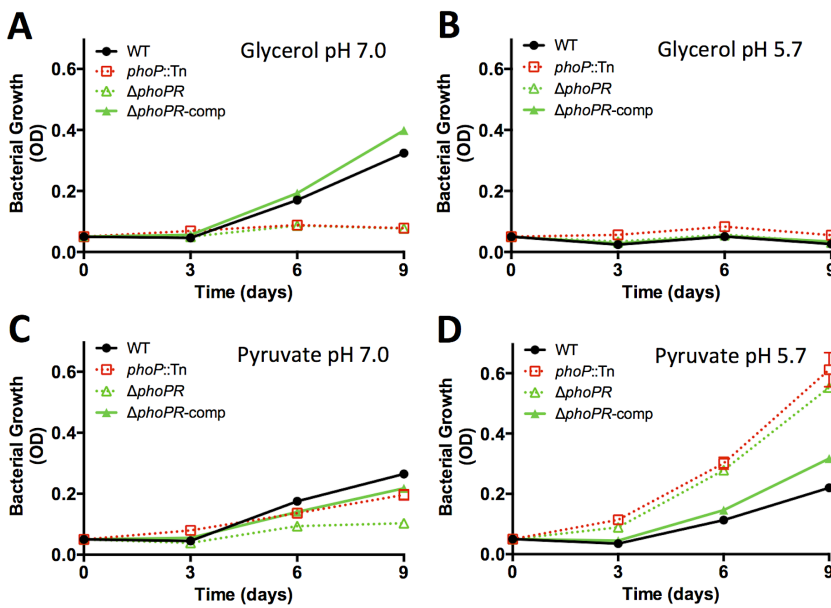


Fig. 3. *phoPR* is required to slow *Mtb* growth at acidic pH. Growth of WT, *phoP*::Tn mutant, Δ *phoPR* mutant, and Δ *phoPR* complemented strains in minimal medium containing 10 mM glycerol at pH 7.0 (A), 10 mM glycerol at pH 5.7 (B), 10 mM pyruvate at pH 7.0 (C), and 10 mM pyruvate at pH 5.7 (D) as a single carbon source. Note that at neutral pH the strains lacking *phoP* have reduced growth on pyruvate and glycerol as compared to the WT or complemented strains. At pH 5.7, strains lacking *phoP* have enhanced growth on pyruvate, as compared to the WT and complemented strains. Error bars represent the standard deviation and the data are representative of three biological replicates.

phoP is required to slow growth in response to acidic pH

Mtb begins to slow its growth in minimal medium with glycerol at pH 6.4, the same pH threshold at which the *phoPR* regulon is induced by acidic pH (Abramovitch *et al.*, 2011). The *phoPR* regulon is strongly induced at pH 5.7 and differentially regulates genes associated with carbon and lipid metabolism (Walters *et al.*, 2006; Gonzalo-Asensio *et al.*, 2008; Abramovitch *et al.*, 2011). Therefore, we hypothesized that *phoPR* may play a role in carbon source-dependent growth arrest. To explore this hypothesis, we examined the response of a CDC1551 *phoP* transposon mutant (*phoP*::Tn; Abramovitch *et al.*, 2011), a *phoPR* deletion mutant and the complemented mutant (Δ *phoPR* and Δ *phoPR* comp; Tan *et al.*, 2013) during growth on single carbon sources at acidic pH. Unexpectedly, at pH 7.0, the Δ *phoPR* mutant exhibited impaired growth on glycerol and pyruvate as single carbon sources as compared to the WT and complemented Δ *phoPR* mutant (Fig. 3A and C). Therefore, *phoPR* is required for growth in medium with glycerol or pyruvate as single carbon sources at neutral pH. At pH 5.7, the *phoP* mutants maintained arrested growth on glycerol (Fig. 3B); however, the *phoP* mutants exhibited significantly enhanced growth on pyruvate as compared to wild-type *Mtb* (Fig. 3D). The enhanced growth on pyruvate at pH 5.7 was complemented in the Δ *phoPR* mutant. The ability of the *phoP* mutants to grow better on pyruvate at acidic pH than at neutral pH is an important observation for several reasons. This finding demonstrates that acidic pH, in a *phoP*-independent manner, remodels *Mtb* physiology to allow growth on pyruvate, and makes available physiological pathways that are inaccessible at neutral pH. It is also

notable that following these adaptations, the Δ *phoPR* mutant exhibits faster growth on pyruvate at pH 5.7 than the WT in any other tested growth condition. This finding shows that *phoPR* functions to slow growth at acidic pH and, thus, explains why reduced growth and induction of the *phoPR* regulon are so closely associated (Abramovitch *et al.*, 2011).

Acidic pH, carbon source and phoP modulate redox homeostasis

The involvement of *phoPR* in the control of growth in response to changes in pH and carbon metabolism suggests that genes of the *phoPR* regulon play a role in modulating growth. Several genes in the *phoPR* regulon, including *pks2*, *pks3*, *pks4*, and *aprA* have been proposed to control redox homeostasis in *Mtb* (Singh *et al.*, 2009; Abramovitch *et al.*, 2011). In this model, under conditions that cause an accumulation of reduced cofactors, such as NADH or NADPH, *Mtb* synthesizes long chain fatty acids using the NADPH consuming fatty acid synthase 1 (*fas*) enzyme to replenish pools of oxidized cofactors (Singh *et al.*, 2009; Farhana *et al.*, 2010). Long chain fatty acids can then be used for the generation of storage lipids such as TAG and *phoP*-dependent cell envelope-associated lipids such as sulpholipid. Given this model, we hypothesized that changes in cytoplasmic redox homeostasis may be associated with pH-, carbon source- and *phoP*-dependent growth arrest.

To characterize the role of redox homeostasis in growth arrest, we examined cytoplasmic redox potential using an *Mtb* strain expressing a redox-sensitive GFP (roGFP). roGFP exhibits ratiometric changes in the excitation

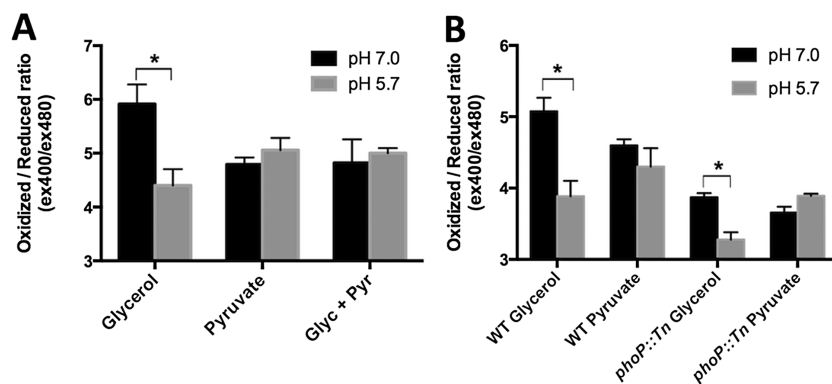


Fig. 4. Acidic pH, carbon source and *phoP* modulate redox homeostasis. Intracellular redox state was measured using a redox-sensitive disulphide bond-containing GFP (roGFP) by calculating the ratio of fluorescence emission from 400 nm and 480 nm excitation. A lower ratio indicates a more reduced roGFP while a higher ratio indicates a more oxidized roGFP.
 A. WT Mtb growing on glycerol exhibits a more reduced cytoplasm at acidic pH. However, when pyruvate is present, Mtb does not exhibit a shift in cytoplasmic redox potential.
 B. The *phoP*::Tn mutant exhibits a more reduced cytoplasm, as compared to the wild type, at pH 7.0 when grown on both glycerol and pyruvate. At pH 5.7, the *phoP* mutant exhibits an even more reduced cytoplasm in glycerol, while maintaining its redox potential in pyruvate. Error bars indicate the standard deviation of three biological replicates each calculated from the average of three technical replicates. The data are representative of two individual experiments. * $P < 0.05$ using a Student's *t*-test.

wavelength based on the redox state of its disulphide bonds and thus provides a measure of cytoplasmic redox potential (Hanson *et al.*, 2004; Cannon and Remington, 2006). roGFP has recently been shown to function in Mtb as a reporter of cytoplasmic redox potential (Bhaskar *et al.*, 2014). At pH 5.7, glycerol as a sole carbon source resulted in a decreased roGFP ratio (Fig. 4A and B, i.e. a more reduced intracellular environment) showing that acidic pH in the presence of glycerol causes enhanced thiol reduction and, consequently, a reduced cytoplasmic potential. For the growth-arrested *phoP*::Tn mutant in minimal medium with glycerol at pH 7.0, we observed a reduced cytoplasmic potential that was equal to that of WT Mtb on glycerol at pH 5.7 (Fig. 4B). This finding demonstrates that *phoP* is required to maintain redox homeostasis during growth on glycerol and that growth arrest is associated with reductive stress. The *phoP*::Tn mutant grown with glycerol at acidic pH exhibits an even more strongly reduced cytoplasm (Fig. 4B) demonstrating that PhoP functions to counteract acidic pH-associated reductive stress.

Glycerol-mediated growth arrest at acidic pH is associated with a reduced cytoplasmic potential; therefore, we hypothesized that pyruvate may alleviate acid-mediated reductive stress. When Mtb is grown in pyruvate alone, or glycerol and pyruvate, the redox potential of the cytoplasm remains unchanged at pH 7.0 and 5.7 (Fig. 4A), demonstrating that Mtb does not experience pH-dependent metabolic stress in the presence of pyruvate. Notably, the *phoP*::Tn mutant grown on pyruvate as a single carbon source exhibits slow growth at neutral pH and enhanced growth at acidic pH; however, the redox potential in both cases was similar to that of growth-arrested Mtb grown on

glycerol at pH 5.7. Therefore, we conclude that a reduced cytoplasmic potential is associated with growth arrest on specific carbon sources, but reductive stress, in the absence of *phoP*, is not sufficient to cause growth arrest. To determine if growth arrest was associated with a shortage of oxidized cofactors, we examined NAD+/NADH and NADP+/NADPH ratios and observed a significant increase in the NAD+/NADH ratio at acidic pH in either 10 mM glycerol or pyruvate and no change in the NADP+/NADPH ratio (Fig. S5). These observations demonstrate that Mtb can maintain a cellular pool of oxidized NAD under conditions of pH-induced reductive stress and that the reduced cytoplasmic potential may be driven by a cytoplasmic redox buffer, such as mycothiol or thioredoxin.

Acidic pH causes transcriptional remodelling of pathways associated with anaplerosis, lipid anabolism, and oxidation of redox cofactors

To explore the mechanisms by which acidic pH remodels Mtb physiology, we undertook RNA-seq-based transcriptional profiling studies. Mtb transcripts were examined following 3-day incubation in minimal medium under four conditions: glycerol pH 7.0, glycerol pH 5.7, pyruvate pH 7.0 and pyruvate pH 5.7. At pH 7.0, only modest transcriptional changes are associated with growth on glycerol or pyruvate, with 61 genes significantly induced (up > 1.5 -fold, $P < 0.05$) and 15 genes significantly repressed in pyruvate as compared to glycerol (Fig. S6A, Table S1). This finding demonstrates limited transcriptional remodelling in response to these carbon sources, perhaps reflecting unrestricted metabolism between glycerol and pyruvate at neutral pH. At acidic pH, substantial tran-

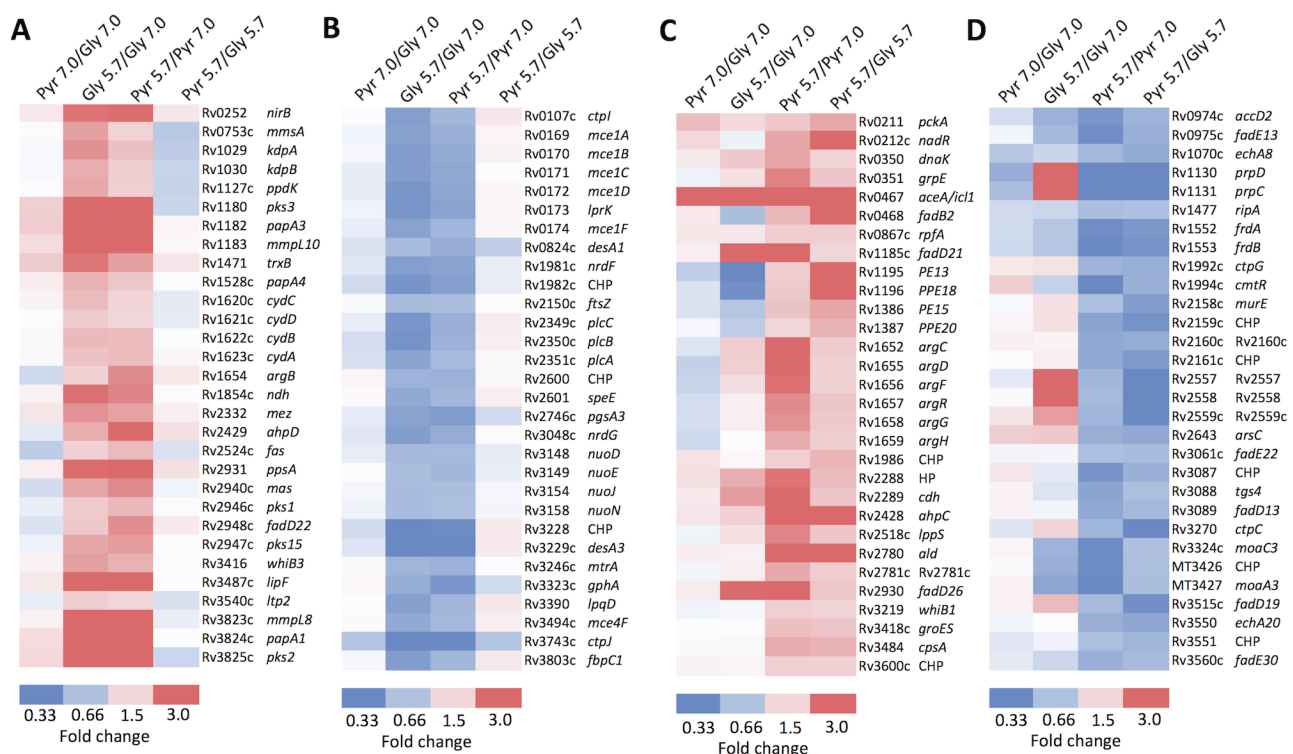


Fig. 5. Genes that are induced or repressed by acidic pH in a carbon source-independent and -dependent manner.

A. Selection of 30 genes (out of 185 total) that are induced by acidic pH in both glycerol and pyruvate without a significant difference in the induction (Table S5A).

B. Selection of 30 genes (out of 134 total) that are repressed by acidic pH in both glycerol and pyruvate without difference in the repression (Table S5C).

C. Selection of 30 genes (out of 60 total) that are induced at pH 5.7 in pyruvate and the induction is significantly greater in pyruvate as compared to glycerol (Table S5B).

D. Selection of 30 genes (out of 75 total) that are repressed at pH 5.7 in pyruvate and the repression is significantly greater in pyruvate as compared to glycerol (Table S5D).

CHP, conserved hypothetical protein; HP hypothetical protein.

scriptional remodelling is observed in both glycerol and pyruvate, with hundreds of genes exhibiting significant differential regulation (Fig. S6B and C, Tables S2 and S3). In contrast to pH 7.0, a direct comparison of transcriptional profiles between pyruvate and glycerol at pH 5.7 revealed 275 and 502 genes with differentially induced or repressed expression respectively (Fig. S6D and Table S4). Overall, these findings support that acidic pH and carbon source, together, promote substantial remodelling of *Mtb* physiology.

Previous attempts to characterize pH-regulated genes have been complicated by the association of acidic pH with a strong downregulation of growth and induction of the stress response, thus making it difficult to separate the genes that are specifically responding to pH, from those associated with a shift in growth and stress status (Fisher *et al.*, 2002; Abramovitch *et al.*, 2011). Comparisons of the RNA-seq profiles identified genes with pH-dependent, carbon source-independent differential expression, with 185 acid-induced genes (Fig. 5A, Fig. S7A, Table S5A) and

134 acid-repressed genes (Fig. 5B, Fig. S7B, Table S5C). These genes represent the *Mtb* pH-dependent regulon that is independent of growth status. The induced genes are highly represented in pathways associated with carbon metabolism and redox homeostasis. For example, many genes of the *phoPR* regulon (Walters *et al.*, 2006; Gonzalo-Asensio *et al.*, 2008; Abramovitch *et al.*, 2011) are strongly induced by acidic pH in both glycerol and pyruvate: *pks2-mmpL8* locus, *pks3-mmpL10* locus, malate dehydrogenase (*mez*) and NADH dehydrogenase (*ndh*). Additionally, several genes without evidence of *phoP*-dependent regulation are induced by acidic pH in both glycerol and pyruvate, including fatty acid synthase (*fas*), PDIM synthesis (*ppsA-ppsE*), pyruvate phosphate dikinase (*ppdK*), and thioredoxin reductase (*trxB*). These acid regulated genes are associated with the regulation of *Mtb* carbon metabolism, lipid anabolism, and replenishment of oxidized cofactors and are consistent with a model where acidic pH is remodelling carbon metabolism to produce lipids and oxidize redox cofactors (Fig. S8).

An additional goal of performing these transcriptional studies was to identify the mechanisms by which pyruvate remodels physiology at acidic pH. Transcriptional profiles consistent with pyruvate- and acidic pH-specialized expression are predicted to exhibit (i) differential expression in pyruvate at pH 5.7 as compared to pH 7.0 (Fig. S6C) and (ii) differential expression in pyruvate as compared to glycerol at pH 5.7 (Figs S6D and S7A and B). For example, genes that are induced in pyruvate and glycerol at pH 5.7, but exhibit enhanced induction in pyruvate are exhibiting pyruvate- and pH-specialized induction. We identified 16 genes with this profile (Fig. 5C and Fig. S7A). Genes exhibiting pyruvate and pH-specialized induction were also identified that are stable in glycerol at pH 5.7 (31 genes) and that are repressed in glycerol at pH 5.7 (13 genes), for a total of 60 genes that are induced in a pyruvate- and pH-specialized manner (Fig. 5C, Fig. S7A, Table S5B). Using a similar analysis we identified 75 genes that are repressed in a pyruvate- and pH-specialized manner (Fig. 5D and Fig. S7B, Table S5D). Genes were also regulated in a glycerol- and pH-specialized manner, with 46 genes and 26 genes showing enhanced induction or repression in glycerol at acidic pH respectively (Fig. S7A and B, Table S5E and F).

The transcriptional profiling data provide additional support for the hypothesis that *Mtb* promotes metabolism around the anaplerotic node at acidic pH (Fig. 1A, Fig. S2). Many of the genes that are most strongly induced in a pyruvate- and pH-specialized manner are associated with the anaplerotic node, including phosphoenolpyruvate carboxykinase (*pckA*) and isocitrate lyase (*icl1*, Fig. 5C, Fig. S7C). *pckA* links the TCA cycle to glycolysis via the reversible metabolism of oxaloacetate to PEP and *icl1* acts as a bypass of an oxidative branch of the TCA cycle via the glyoxylate shunt. *pckA* and *icl1* exhibit induction by pyruvate at pH 7.0 and further induction by acidic pH in both glycerol and pyruvate, with the result of twofold and fourfold induction in pyruvate as compared to glycerol at pH 5.7 respectively. These findings are fully consistent with our growth studies and reinforce that acidic pH and pyruvate promote metabolism around the PEP-pyruvate-oxaloacetate node. The observation of *icl1* induction at acidic pH is also consistent with prior observations under different pH stress conditions (Fisher *et al.*, 2002; Rohde *et al.*, 2007). *Icl* also functions as a methylisocitrate lyase that is required for the methylcitrate cycle and *Mtb* growth on single carbon sources such as acetate and propionate (Eoh and Rhee, 2014). Therefore, it is interesting that the methyl citrate cycle is strongly repressed in a pH- and pyruvate specialized manner, with methyl citrate synthase (*prpC*) and methylcitrate dehydratase (*prpD*) both being downregulated ~ 29-fold in pyruvate compared to glycerol at pH 5.7. This strong difference is the result of *prpCD* being induced by acidic pH in glycerol, but repressed in

pyruvate (Fig. 5D). The divergent regulation of the methyl citrate cycle further supports pH-dependent modulation of central carbon metabolism and may have consequences for the metabolism of cholesterol during pathogenesis.

Acidic pH remodels *Mtb* lipid and central carbon metabolism

The transcriptional profiling data identified widespread induction of genes associated with lipid metabolism. For example, in both glycerol and pyruvate at pH 5.7, the *mmpL8-pks2* operon (Rv3823c–Rv3825c) is strongly induced (Fig. 5A). This operon has been shown to control the synthesis of sulpholipid (Sirakova *et al.*, 2001) in a *phoPR*-dependent manner (Asensio *et al.*, 2006; Walters *et al.*, 2006). Therefore, it is predicted that sulpholipid should accumulate at acidic pH. To test this prediction, *Mtb* was grown in minimal medium amended with 10 mM pyruvate buffered at pH 7.0 and pH 5.7. The culture was incubated for 3 days, to enable the cultures to become pH-adapted, and the lipids were then radiolabelled with a trace amount of ¹⁴C acetate. As predicted, in wild-type *Mtb*, sulpholipids were induced approximately threefold at pH 5.7 as compared to pH 7.0 (Fig. 6A, Fig. S9A and C). The *ΔphoPR* mutant did not accumulate sulpholipids and this phenotype was complemented (Fig. 6A, Fig. S9C). Therefore, acidic pH remodels lipid metabolism by stimulating *PhoPR* and promoting the accumulation of sulpholipid.

One proposed role for the synthesis of *phoPR*-dependent lipids is to consume reductants and relieve reductive stress (Singh *et al.*, 2009; Farhana *et al.*, 2010). This model is supported by our roGFP studies (Fig. 4B), where the *phoP*::Tn mutant has a more reduced cytoplasm. Based on the reductive stress model, it is predicted that the *ΔphoPR* mutant may accumulate other long chain fatty acids to compensate for the loss of *phoPR*-dependent lipids. Indeed, enhanced PDIM accumulation has previously been observed in the *phoP*::Tn mutant (Abramovitch *et al.*, 2011) and, conversely, a loss of PDIM causes an accumulation of sulpholipid (Jain *et al.*, 2007). When grown on pyruvate, relatively low levels of radiolabelled PDIM are observed in all of the tested strains or conditions (Fig. S9B); however, TAG accumulation is induced approximately threefold in WT *Mtb* at pH 5.7 and approximately sixfold in the *phoPR* mutant (Fig. 6B, Fig. S9C). Therefore, *Mtb* accumulates both TAG and sulpholipid at acidic pH, and in the absence of *phoPR* and sulpholipid, compensates by increasing the accumulation of TAG.

Our data support that environmental pH acts as a checkpoint on *Mtb* metabolism and that acidic pH restricts some metabolic pathways while making new pathways available to the bacterium. Indeed, the *phoPR* mutant exhibits restricted growth on pyruvate at pH 7.0 and substantially enhanced growth at pH 5.7 (Fig. 3), strongly supporting

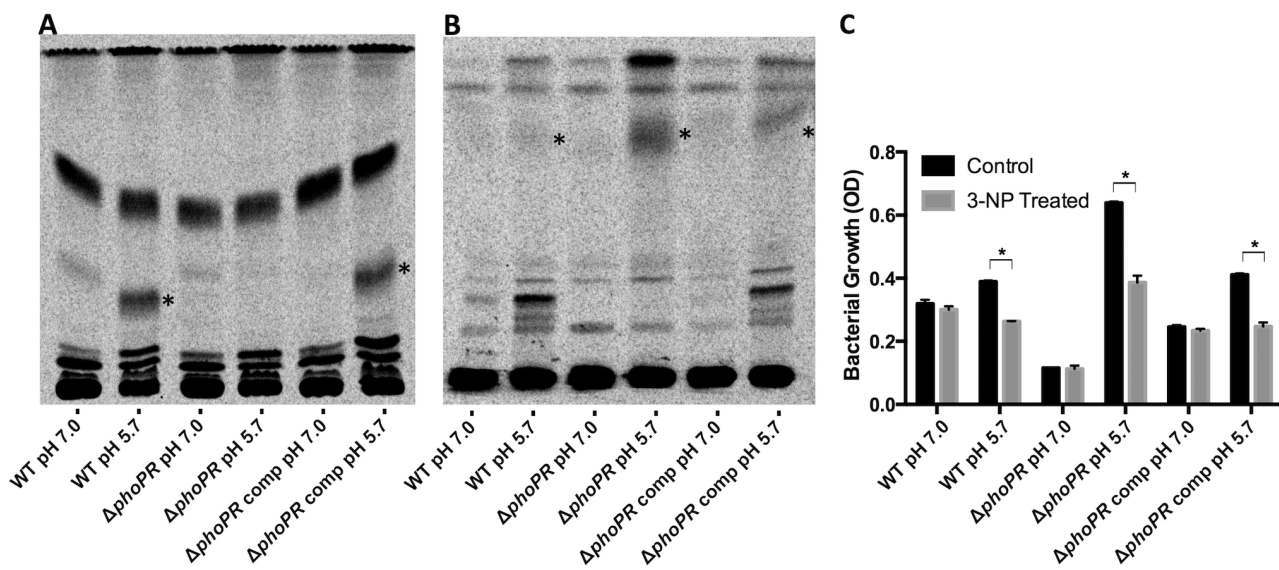


Fig. 6. Acidic pH modulates accumulation of mycobacterial lipids and sensitivity to 3-NP.

A. Accumulation of sulpholipid at acidic pH. For each strain, 20 000 CPM of ^{14}C labelled lipids was spotted at the origin and the TLC was developed three times in chloroform:methanol:water (90:10:1 v/v/v). Sulpholipid is highlighted with the asterisk and accumulates in a pH- and *phoPR*-dependent manner.

B. Accumulation of TAG in the *phoPR* mutant at acidic pH. For each strain, 20 000 CPM of ^{14}C labelled lipids was spotted at the origin and the TLC was developed in hexane:diethyl ether:acetic acid (80:20:1 v/v/v). TAG is highlighted with the asterisk and accumulates in a pH- and *phoPR*-dependent manner. The data are representative of two independent biological replicates.

C. 3-NP inhibits *Mtb* growth at acidic pH. The data presented are the end-point of culture growth following 9 days of incubation at acidic or neutral pH in the presence or absence of 0.1 mM 3-NP. Data showing the entire time-course are presented in Fig. S10. Error bars represent the standard deviation and the data are representative of two biological replicates. * $P < 0.005$ using a Student's *t*-test.

that acidic pH makes new metabolic avenues available to the pathogen. We hypothesized that the glyoxylate shunt or methylcitrate cycle may be promoted at acidic pH, based on the strong induction of *icl1* at acidic pH (Fig. 5C) and the requirement of carbon sources that fuel the anaplerotic node for growth at acidic pH (Fig. 1A). To test this hypothesis, the effect of the isocitrate lyase inhibitor 3-nitropropionic acid (3-NP) was tested on *Mtb* grown on pyruvate at pH 7.0 and 5.7. In wild-type *Mtb*, a significant ~30% reduction of growth was observed at acidic pH in the presence of 3-NP (Fig. 6C, Fig. S10). No change in growth was observed at neutral pH, suggesting that *icl1* is required in a pH-dependent manner. In the *ΔphoPR* mutant, we observed a similar 40% decrease in growth caused by the addition of 3-NP. Notably, almost all of the enhanced growth observed in the *ΔphoPR* mutant at acidic pH is inhibited by 3-NP (Fig. 6C). Therefore, acidic pH, in a *phoP*-independent manner, promotes metabolism through a 3-NP-sensitive pathway, such as the glyoxylate shunt or methylcitrate cycle.

Discussion

We have shown that acidic pH alone does not slow *Mtb* growth. When supplied an appropriate carbon source, such as pyruvate, or in the absence of *phoPR*, *Mtb* grows

about as well, or better, at acidic pH as compared to neutral pH. This reveals that slow growth at acidic pH is regulated by available carbon sources and signal transduction-dependent transcriptional remodelling (Fig. 7). Additional studies examining the mechanisms of slowed growth at

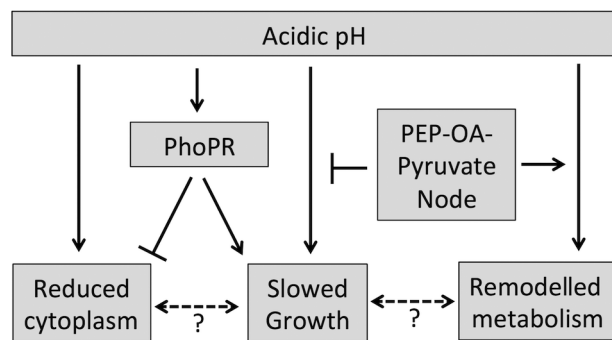


Fig. 7. Schematic diagram summarizing the role of acidic pH in regulating growth and redox homeostasis. Acidic pH drives a reduction of the cytoplasmic potential and a slowing of *Mtb* growth. PhoPR functions to mitigate reductive stress and slow *Mtb* growth. This is possibly achieved by syphoning carbon away from the TCA cycle to promote oxidation of NADPH through lipid anabolism, such as acid inducible sulpholipid accumulation (Fig. 6A). Addition of PEP-oxaloacetate- pyruvate node metabolites may promote growth by fuelling the TCA cycle and remodelling central metabolism, including the induction of *pckA* and *icl1*.

acidic pH demonstrate that *Mtb* exhibits a reduced cytoplasm, promotes the synthesis of sulpholipid, and induces expression of genes associated with anaplerotic metabolism. Together, these findings support that *Mtb* can link pH and available carbon sources as environmental cues to regulate its growth and metabolism. During infection, this physiological adaptation may enable *Mtb* to survive in microenvironments that are otherwise inhospitable for microbial colonization.

We have identified two distinct branches of pH-driven adaptation: a *phoPR*-dependent branch and *phoPR*-independent branch (Fig. 7). The *phoPR*-dependent branch plays a role in maintaining redox homeostasis and slowing growth. In glycerol, acidic pH causes a reduced cytoplasmic potential that is associated with slowed growth and induction of the *phoPR* regulon. Notably, the Δ *phoPR* mutant grows poorly at pH 7.0 on glycerol or pyruvate, carbon sources that are permissive for growth of WT *Mtb* at neutral pH (Fig. 3). This growth arrest is associated with a reduction of the cytoplasmic potential (Fig. 4B), demonstrating that *phoPR* is required for redox homeostasis and growth on glycerol or pyruvate. A possible mechanism for *phoPR*-dependent maintenance of redox homeostasis is the production of methyl-branched lipids such as sulpholipid. Anabolism of these lipids would oxidize NADPH as well as reduce flux through the TCA cycle, thus decreasing the production of NADH. Consistent with this model, we observe that sulpholipid accumulates in a pH- and *phoPR*-dependent manner (Fig. 6A). In the absence of *phoPR*, *Mtb* accumulates TAG at acidic pH, possibly to compensate for a loss of *phoPR*-dependent lipid anabolism (Fig. 6B). Similarly, Singh and colleagues have also observed that a *whiB3* mutant, which is defective in synthesis of sulpholipid, experiences reductive stress and enhanced TAG accumulation (Singh *et al.*, 2009). Thus, we propose that *phoPR* may cause slow growth at acidic pH by syphoning carbon towards lipid anabolism as part of its function to maintain redox homeostasis.

The response of the Δ *phoPR* mutant to acidic pH also supports a role for *phoPR*-independent mechanisms of pH-driven adaptation. The dramatic shifts in growth phenotypes of the Δ *phoPR* mutant in pyruvate at pH 5.7 (enhanced growth) as compared to pH 7.0 (restricted growth) support that *phoPR*-independent remodelling of metabolism promotes growth at acidic pH on select carbon sources. This hypothesis is supported by the observations that at acidic pH: (i) addition of 3-NP, an inhibitor of *icl*, decreases the enhanced growth observed in the Δ *phoPR* mutant (Fig. 6C), (ii) *icl1* and *pckA* expression is induced (Fig. 5C), and (iii) *Mtb* favours carbon sources feeding the anaplerotic node (Fig. 1A). The inhibitory effect of 3-NP on the enhanced growth and induction of *icl1* expression supports that the glyoxylate shunt or methylcitrate cycle may be one of the induced metabolic pathways that

become available to *Mtb* at acidic pH. Eoh and Rhee have shown that, when *Mtb* is grown on glucose or propionate, disruption of *icl* causes decreased cytoplasmic pH, imbalanced NAD+/NADH ratios and an altered membrane potential (Eoh and Rhee, 2014). Therefore, induction of *icl* at acidic pH may function to promote metabolism that maintains pH- and redox-homeostasis.

The presented growth, genetic and lipid metabolism studies support a model whereby carbon metabolism is remodelled by acidic pH. Transcriptional profiling experiments reveal that several key genes of central metabolism are induced by acidic pH. Most notably, *pckA* and *icl1* are strongly induced by both acidic pH and pyruvate. Munoz-Elias and McKinney have suggested that *pckA* and *icl1*, which are both essential for growth in animals (McKinney *et al.*, 2000; Munoz-Elias and McKinney, 2005; Marrero *et al.*, 2010), may be required for virulence to promote metabolism via the PEP-glyoxylate cycle (Munoz-Elias and McKinney, 2006). The PEP-glyoxylate cycle has been observed in *Escherichia coli* during slow growth on glucose limiting medium and enables the full oxidation of carbon sources that fuel the anaplerotic node (Fischer and Sauer, 2003), such as pyruvate or acetyl-CoA. During *Mtb* infection, these carbon sources are physiologically relevant as they are the products of cholesterol or fatty acid catabolism. In this manner, the PEP-glyoxylate cycle may promote efficient energy producing catabolism, while keeping PEP, pyruvate, oxaloacetate and acetyl-CoA abundant and available for anabolism. Studies from others provide support for this model. For example, Beste and colleagues have shown using ^{13}C -metabolic flux analysis that during slow growth in a chemostat or growth in macrophages *Mtb* exhibits anaplerotic carbon flux through *pckA*- and *icl1*-dependent pathways (Beste *et al.*, 2011; 2013). Additionally, both *pckA* and *icl1* are upregulated during 2 weeks of growth in macrophages (Rohde *et al.*, 2012) and 50 days of growth in mice (Timm *et al.*, 2003; Shi *et al.*, 2010), demonstrating this physiology is relevant in the context of pathogenesis and may be driven by the combined influence of environmental pH and available carbon sources in animals. Together, these data support a model where acidic pH: (i) induces *phoP*-dependent lipid anabolism to oxidize redox cofactors and slow growth by diverting carbon from central metabolism, and (ii) drives *Mtb* physiology to adopt the PEP-glyoxylate cycle, to balance energy production and carbon utilization (Fig. S8).

Redox homeostasis was found to play an important role in pH-driven adaptation. The reduced cytoplasmic potential observed at acidic pH (Fig. 4) may be the result of decreased oxidative phosphorylation where acidic pH restricts the efficiency of proton-pumping enzymes in the electron transport chain. In this manner, growth at acidic pH has parallels with hypoxia-driven adaptation, where oxidative phosphorylation is limited due to decreased

oxygen as a terminal electron acceptor (Boshoff and Barry, 2005). However, we observed limited pH-dependent changes in the concentration of NAD⁺ or NADP⁺ (Fig. S5), demonstrating that Mtb has physiological mechanisms to regenerate oxidized cofactors. Transcriptional profiling experiments provide insights into potential mechanisms of pH-dependent redox homeostasis. Acidic pH, independent of carbon source, causes the induction of the *phoPR* regulon, fatty acid synthase (*fas*), PDIM, and *whiB3* genes that would promote lipid anabolism and oxidize NADPH (Singh *et al.*, 2009; Lee *et al.*, 2013). Several additional genes induced at acidic pH are predicted to be associated with replenishing oxidized cofactors (Fig. S8), including *ahpCD* (Bryk *et al.*, 2002), NADH dehydrogenase (*ndh*; Vilchez *et al.*, 2005), and thioredoxin reductase (*trxB*; Akif *et al.*, 2008). Another mechanism of redox homeostasis is the use of thiols, including mycothiol (Vilchez *et al.*, 2008), as reductive sinks. roGFP measures redox potential via a thiol-based mechanism providing direct evidence for increased thiol reduction at acidic pH or in the *phoP* mutant (Fig. 4). The mycothiol redox couple oxidizes NADPH and therefore, in combination with mechanisms considered above, may be an important redox buffer at acidic pH. These findings suggest that promoting lipid anabolism and redox cofactor oxidation at acidic pH may be important transcriptional adaptations.

Carbon source-specific growth arrest in response to acidic pH appears to be a pathogenesis associated and evolved trait in Mtb, as the non-pathogen *M. smegmatis* does not share this physiology (Fig. S4). It is possible that, as part of pathogenesis, Mtb is integrating signals from environmental pH and available carbon sources to adapt to specific host microenvironments. Therefore, acidic pH may restrict Mtb from metabolizing specific carbon sources *in vivo*, and require carbon sources feeding the anaplerotic node, such as cholesterol, as a checkpoint for growth and pathogenesis. *phoP*, *pckA* and *icl1* are required for virulence in animals (McKinney *et al.*, 2000; Perez *et al.*, 2001; Munoz-Elias and McKinney, 2005; Marrero *et al.*, 2010), suggesting that this pH-driven response is important during pathogenesis. *phoP* mutants are attenuated for virulence and one demonstrated mechanism for this attenuation is decreased ESAT-6 secretion (Frigui *et al.*, 2008). Notably, in primary human macrophages, deletion of genes required to synthesize *phoPR*-regulated lipids such as sulpholipid, diacyl- and polyacyltreholose (e.g. *pks2*, *pks3* and *pks4*), results in a macrophage growth defect in the absence of PDIM (Passemar *et al.*, 2014), suggesting that PDIM synthesis may compensate as a reductive sink during macrophage infection and that *phoPR*-regulated, pH-inducible lipids such as sulpholipid play a role in pathogenesis. It is possible that the inability of the *phoP* mutant to modulate redox homeostasis or metabolically constrain Mtb growth in response to acidic pH may

also account, in part, for the attenuation of the *phoP* mutant observed in macrophages and animals (Perez *et al.*, 2001).

Experimental procedures

Bacterial strains and growth conditions

All Mtb experiments, unless otherwise stated, were performed with Mtb strain CDC1551. The *phoP*:Tn and *ΔphoPR* mutants have been previously described (Abramovitch *et al.*, 2011; Tan *et al.*, 2013). Cultures were maintained in 7H9 Middlebrook medium supplemented with 10% OADC and 0.05% Tween-80. All single carbon source experiments were performed in a defined minimal medium as described by Lee *et al.* (2013): 1 g l⁻¹ KH₂PO₄, 2.5 g l⁻¹ Na₂PO₄, 0.5 g l⁻¹ (NH₄)₂SO₄, 0.15 g l⁻¹ asparagine, 10 mg l⁻¹ MgSO₄, 50 mg l⁻¹ ferric ammonium citrate, 0.1 mg l⁻¹ ZnSO₄, 0.5 mg l⁻¹ CaCl₂, and 0.05% Tyloxapol. Media was buffered using 100 mM MOPS (pH 6.6–7.0) or MES (pH 5.7–6.5) (Piddington *et al.*, 2000). Following 9 days of Mtb growth, the pH of the medium was tested and there were no significant changes to the pH, demonstrating the strong buffering is sufficient to counteract Mtb modulation of media pH. For 9-day growth experiments, Mtb was seeded in T-25 standing tissue culture flasks in 8 ml of minimal medium at an initial density of 0.05 OD₆₀₀ and incubated at 37°C and 500 µl samples were removed every 3 days for optical density measurements. The 36-day growth experiments were performed as described for the 9 days experiments, except that 250 µl of culture was removed for optical density measurements at each time point. Over the 36-day time-course, pH was measured at each time point using pH strips sensitive to 0.3 pH units and no changes were observed. At the final day, the pH of the supernatants was measured using a pH meter, and only minimal (< 0.2 units) changes in pH were observed (Fig. S3B). 3-NP was used at 0.1 mM. Growth of *M. smegmatis* mc2155 was performed as described for Mtb.

Cytoplasmic pH measurement

Cytoplasmic pH was measured using the pH-sensitive dye CMFDA as described previously by Purdy *et al.* (2009). Briefly, Mtb was inoculated into its respective conditions at an original OD of 0.05. After 3 days, samples were collected, pelleted, and resuspended in 500 µl of the same minimal media. Four microlitres of 1 µg ml⁻¹ CMFDA dye was added to each sample and incubated at 37°C for 2 h. Samples were then washed twice, resuspended at OD 1.2 in the same medium, and transferred to a 96-well microplate. A standard curve was prepared using Mtb in buffered minimal media treated with 10 µM nigericin. Fluorescent emission was measured at 520 nm after excitation at 450 nm and 490 nm.

Measuring intracellular redox poise

The plasmid pVV-16 was modified to constitutively express a redox-sensitive GFP roGFP-R12 (Cannon and Remington, 2006). This construct was transformed into the CDC1551 background. Mtb was cultured in the indicated media containing 10 mM of the carbon source at a starting OD of 0.3. For each experimental condition, CDC1551 containing an empty

vector was also cultured to use as a control for background signal subtraction. On day 3, 200 µl of each treatment was transferred in triplicate to a 96-well microplate and fluorescence emission was read at 510 nm after excitation at 400 nm and 480 nm, measuring the relative abundance of the oxidized and reduced roGFP species respectively.

RNA-seq transcriptional profiling and data analysis

Mtb cultures were grown at 37°C in T-75 vented, standing tissue culture flasks in 40 ml of a defined minimal medium seeded at an initial OD of 0.1. Four conditions were examined with two biological replicates: (i) 10 mM Glycerol, pH 7.0, (ii) 10 mM Glycerol pH 5.7, (iii) 10 mM Pyruvate pH 7.0 and (iv) 10 mM Pyruvate pH 5.7. Following a 3-day incubation, total bacterial RNA was stabilized and extracted as previously described (Rohde *et al.*, 2007). RNA quality and integrity were examined using an Agilent Bioanalyser prior to subjecting samples to rRNA depletion using the Epicentre Ribo-Zero depletion kit. cDNA libraries were constructed using the Illumina TruSeq RNA library preparation kit (v2), omitting the polyA selection step. After library quality control, sample libraries were pooled and sequenced in one lane of an Illumina HiSeq 2500 Rapid Run flow cell (v1) in 50bp, single-end read format (SE50). After the sequencing run, reads were de-multiplexed and converted to FASTQ format using the Illumina bcl2fastq (v1.8.4) script. The reads in the raw data files were then subjected to trimming of low-quality bases and removal of adapter sequences using Trimmomatic (v0.30) (Lohse *et al.*, 2012) with a 4 bp sliding window, cutting when the read quality dropped below 15 or read length was less than 36 bp. Trimmed reads were aligned to the *Mtb* CDC1551 genome (NCBI accession AE000516) using Bowtie (Langmead *et al.*, 2009) with the -S option to produce SAM files as output. SAM files produced by Bowtie were converted to BAM files and coverage depth was calculated using SAMtools (Li *et al.*, 2009) resulting in > 98% coverage across the genome with an average of 172× coverage (ranging between 110× and 211× depending on the sample). Aligned reads were then counted per gene feature in the *Mtb* CDC1551 genome using the HTSeq software suite. Data were normalized by estimating effective library sizes using robust regression within the DESeq package (Anders and Huber, 2010). Statistical analysis and differential gene expression was performed in RStudio (V0.97.551) by fitting a negative binomial model to each set of conditions and testing for differences utilizing the DESeq package. The Magnitude-Amplitude (MA) plots were generated by modifying a function in DESeq and plotting the average expression of differentially expressed genes from each set of conditions tested against the expression ratio. For each comparison (Fig. S6A–D, supplemental Tables S1–S4), differentially expressed genes were identified as genes with an average normalized count > 100, differential gene expression > 1.5-fold, and a *P*-value < 0.05. Venn diagrams were generated using the Venny web tool (<http://bioinfogp.cnb.csic.es/tools/venny/>). Two biological replicates were performed for each sample and analysis using QualiMap (Garcia-Alcalde *et al.*, 2012) demonstrated excellent agreement between biological replicates with a Pearson's correlation coefficient of ~ 1. The transcriptional profiling data have been submitted to the NCBI GEO database (Accession No.

GSE52020). RNA-seq expression data for *pk2*, *ic1*, and *pckA* was confirmed using quantitative real-time PCR and previously described methods (Abramovitch *et al.*, 2011). The acidic pH induction of *pk2* was confirmed to be carbon source independent, and acidic pH induction of *ic1* and *pckA* was confirmed to be enhanced in pyruvate (Fig. S7C).

Analysis of mycobacterial lipids

For lipid analysis, bacterial cultures were grown as described above for the transcriptional profiling experiments. Two conditions were examined: (i) 10 mM pyruvate pH 7.0 and (ii) 10 mM pyruvate pH 5.7. Following 3-day incubation, lipids were radiolabelled by adding 8 µCi of [1,2¹⁴C] sodium acetate to each culture. The final concentration of acetate used for the labelling is 200 µM, a concentration 50-fold lower than the 10 mM pyruvate. Following 6 days of labelling, the bacteria were pelleted, washed in PBS and the lipids were extracted twice in 2:1 chloroform methanol and Folch washed. ¹⁴C incorporation was determined by scintillation counting of the total extractable lipids. To analyse lipid species, 20 000 counts per minute (CPM) of the lipid sample was spotted at the origin of 100 cm² silica gel 60 aluminium sheets. To separate sulfolipid for quantification, the TLC was analysed with the chloroform:methanol:water (90:10:1 v/v/v) solvent system (Asensio *et al.*, 2006). To separate TAG for quantification, the TLC was developed with hexane:diethyl ether:acetic acid (80:20:1, v/v/v) solvent system (Abramovitch *et al.*, 2011). To examine PDIM accumulation the TLC was developed in petroleum ether:acetone (98:2 v/v). Radiolabelled lipids were detected and quantified using a phosphor screen and a Storm Imager and ImageJ software (Schneider *et al.*, 2012). Radiolabelling experiments, lipid extractions and TLCs were repeated in two independent biological replicates with similar findings in both replicates.

Acknowledgements

We are grateful to the Remington laboratory for providing the roGFP gene, Christopher Colvin for technical assistance, the MSU RTSF for RNA-seq library preparation and sequencing, and Kathy Meek, Martha Mulks, Kyle Rohde and members of the Abramovitch lab for critical reading of the manuscript. The High Performance Computing Cluster and iCER at Michigan State University provided computational support and resources. This research was supported by start-up funding from Michigan State University, AgBioResearch and a Career Development Grant from the Great Lakes Regional Center of Excellence (National Institute of Allergy and Infectious Disease Award U54 AI057153).

References

- Abramovitch, R.B., Rohde, K.H., Hsu, F.F., and Russell, D.G. (2011) *aprABC*: a *Mycobacterium tuberculosis* complex-specific locus that modulates pH-driven adaptation to the macrophage phagosome. *Mol Microbiol* **80**: 678–694.
- Akif, M., Khare, G., Tyagi, A.K., Mande, S.C., and Sardesai, A.A. (2008) Functional studies of multiple thioredoxins from *Mycobacterium tuberculosis*. *J Bacteriol* **190**: 7087–7095.
- Anders, S., and Huber, W. (2010) Differential expression

- analysis for sequence count data. *Genome Biol* **11**: R106.
- Asensio, J.G., Maia, C., Ferrer, N.L., Barilone, N., Laval, F., Soto, C.Y., et al. (2006) The virulence-associated two component PhoP–PhoR system controls the biosynthesis of polyketide-derived lipids in *Mycobacterium tuberculosis*. *J Biol Chem* **281**: 1313–1316.
- Baek, S.H., Li, A.H., and Sassetti, C.M. (2011) Metabolic regulation of mycobacterial growth and antibiotic sensitivity. *PLoS Biol* **9**: e1001065.
- Beste, D.J., Noh, K., Niedenfuhr, S., Mendum, T.A., Hawkins, N.D., Ward, J.L., et al. (2013) (13)C-flux spectral analysis of host–pathogen metabolism reveals a mixed diet for intracellular *Mycobacterium tuberculosis*. *Chem Biol* **20**: 1012–1021.
- Beste, D.J.V., Bonde, B., Hawkins, N., Ward, J.L., Beale, M.H., Noack, S., et al. (2011) C-13 metabolic flux analysis identifies an unusual route for pyruvate dissimilation in mycobacteria which requires isocitrate lyase and carbon dioxide fixation. *PLoS Pathog* **7**: e1002091.
- Bhaskar, A., Chawla, M., Mehta, M., Parikh, P., Chandra, P., Bhave, D., et al. (2014) Reengineering redox sensitive GFP to measure mycothiol redox potential of *Mycobacterium tuberculosis* during infection. *PLoS Pathog* **10**: e1003902.
- Boshoff, H.I., and Barry, C.E., 3rd (2005) Tuberculosis – metabolism and respiration in the absence of growth. *Nat Rev Microbiol* **3**: 70–80.
- Bryk, R., Lima, C.D., Erdjument-Bromage, H., Tempst, P., and Nathan, C. (2002) Metabolic enzymes of mycobacteria linked to antioxidant defense by a thioredoxin-like protein. *Science* **295**: 1073–1077.
- Cannon, M.B., and Remington, S.J. (2006) Re-engineering redox-sensitive green fluorescent protein for improved response rate. *Protein Sci* **15**: 45–57.
- Chang, J.C., Miner, M.D., Pandey, A.K., Gill, W.P., Harik, N.S., Sassetti, C.M., and Sherman, D.R. (2009) *igr* genes and *Mycobacterium tuberculosis* cholesterol metabolism. *J Bacteriol* **191**: 5232–5239.
- Dannenberg, A.M. (2006) *Pathogenesis of Human Pulmonary Tuberculosis: Insights from the Rabbit Model*. Washington DC: ASM Press, pp. 1–453.
- Eoh, H., and Rhee, K.Y. (2014) Methylcitrate cycle defines the bactericidal essentiality of isocitrate lyase for survival of *Mycobacterium tuberculosis* on fatty acids. *Proc Natl Acad Sci USA* **111**: 4976–4981.
- Farhana, A., Guidry, L., Srivastava, A., Singh, A., Hondalus, M.K., and Steyn, A.J.C. (2010) Reductive stress in microbes: implications for understanding *Mycobacterium tuberculosis* disease and persistence. *Adv Microb Physiol* **57**: 43–117.
- Fischer, E., and Sauer, U. (2003) A novel metabolic cycle catalyzes glucose oxidation and anaplerosis in hungry *Escherichia coli*. *J Biol Chem* **278**: 46446–46451.
- Fisher, M.A., Plikaytis, B.B., and Shinnick, T.M. (2002) Microarray analysis of the *Mycobacterium tuberculosis* transcriptional response to the acidic conditions found in phagosomes. *J Bacteriol* **184**: 4025–4032.
- Frigui, W., Bottai, D., Majlessi, L., Monot, M., Josselin, E., Brodin, P., et al. (2008) Control of *M. tuberculosis* ESAT-6 secretion and specific T cell recognition by PhoP. *PLoS Pathog* **4**: e33.
- Galagan, J.E., Minch, K., Peterson, M., Lyubetskaya, A., Azizi, E., Sweet, L., et al. (2013) The *Mycobacterium tuberculosis* regulatory network and hypoxia. *Nature* **499**: 178–183.
- Garcia-Alcalde, F., Okonechnikov, K., Carbonell, J., Cruz, L.M., Gotz, S., Tarazona, S., et al. (2012) Qualimap: evaluating next-generation sequencing alignment data. *Bioinformatics* **28**: 2678–2679.
- Gill, W.P., Harik, N.S., Whiddon, M.R., Liao, R.P., Mittler, J.E., and Sherman, D.R. (2009) A replication clock for *Mycobacterium tuberculosis*. *Nat Med* **15**: 211–214.
- Gonzalo-Asensio, J., Mostowy, S., Harders-Westerveen, J., Huygen, K., Hernandez-Pando, R., Thole, J., et al. (2008) PhoP: a missing piece in the intricate puzzle of *Mycobacterium tuberculosis* virulence. *PLoS ONE* **3**: e3496.
- Hanson, G.T., Aggeler, R., Oglesbee, D., Cannon, M., Capaldi, R.A., Tsien, R.Y., and Remington, S.J. (2004) Investigating mitochondrial redox potential with redox-sensitive green fluorescent protein indicators. *J Biol Chem* **279**: 13044–13053.
- Homolka, S., Niemann, S., Russell, D.G., and Rohde, K.H. (2010) Functional genetic diversity among *Mycobacterium tuberculosis* complex clinical isolates: delineation of conserved core and lineage-specific transcriptomes during intracellular survival. *PLoS Pathog* **6**: e1000988.
- Jain, M., Petzold, C.J., Schelle, M.W., Leavell, M.D., Mougous, J.D., Bertozi, C.R., et al. (2007) Lipidomics reveals control of *Mycobacterium tuberculosis* virulence lipids via metabolic coupling. *Proc Natl Acad Sci USA* **104**: 5133–5138.
- Kim, M.J., Wainwright, H.C., Locketz, M., Bekker, L.G., Walther, G.B., Dittrich, C., et al. (2010) Caseation of human tuberculosis granulomas correlates with elevated host lipid metabolism. *EMBO Mol Med* **2**: 258–274.
- Langmead, B., Trapnell, C., Pop, M., and Salzberg, S.L. (2009) Ultrafast and memory-efficient alignment of short DNA sequences to the human genome. *Genome Biol* **10**: R25.
- Lee, W., Vanderven, B.C., Fahey, R.J., and Russell, D.G. (2013) Intracellular *Mycobacterium tuberculosis* exploits host-derived fatty acids to limit metabolic stress. *J Biol Chem* **288**: 6788–6800.
- Li, H., Handsaker, B., Wysoker, A., Fennell, T., Ruan, J., Homer, N., et al. (2009) The Sequence Alignment/Map format and SAMtools. *Bioinformatics* **25**: 2078–2079.
- Lohse, M., Bolger, A.M., Nagel, A., Fernie, A.R., Lunn, J.E., Stitt, M., and Usadel, B. (2012) RobiNA: a user-friendly, integrated software solution for RNA-Seq-based transcriptomics. *Nucleic Acids Res* **40**: W622–W627.
- McKinney, J.D., Honer zu Bentrup, K., Munoz-Elias, E.J., Miczak, A., Chen, B., Chan, W.T., et al. (2000) Persistence of *Mycobacterium tuberculosis* in macrophages and mice requires the glyoxylate shunt enzyme isocitrate lyase. *Nature* **406**: 735–738.
- Marrero, J., Rhee, K.Y., Schnappinger, D., Pethe, K., and Ehrt, S. (2010) Gluconeogenic carbon flow of tricarboxylic acid cycle intermediates is critical for *Mycobacterium tuberculosis* to establish and maintain infection. *Proc Natl Acad Sci USA* **107**: 9819–9824.
- Martin, C., Williams, A., Hernandez-Pando, R., Cardona, P.J., Gormley, E., Bordat, Y., et al. (2006) The live *Mycobacte-*

- rium tuberculosis* *phoP* mutant strain is more attenuated than BCG and confers protective immunity against tuberculosis in mice and guinea pigs. *Vaccine* **24**: 3408–3419.
- Munoz-Elias, E.J., and McKinney, J.D. (2005) *Mycobacterium tuberculosis* isocitrate lyases 1 and 2 are jointly required for *in vivo* growth and virulence. *Nat Med* **11**: 638–644.
- Munoz-Elias, E.J., and McKinney, J.D. (2006) Carbon metabolism of intracellular bacteria. *Cell Microbiol* **8**: 10–22.
- Munoz-Elias, E.J., Timm, J., Botha, T., Chan, W.T., Gomez, J.E., and McKinney, J.D. (2005) Replication dynamics of *Mycobacterium tuberculosis* in chronically infected mice. *Infect Immun* **73**: 546–551.
- Pandey, A.K., and Sassetti, C.M. (2008) Mycobacterial persistence requires the utilization of host cholesterol. *Proc Natl Acad Sci USA* **105**: 4376–4380.
- Passemar, C., Arbues, A., Malaga, W., Mercier, I., Moreau, F., Lepourry, L., et al. (2014) Multiple deletions in the polyketide synthase gene repertoire of *Mycobacterium tuberculosis* reveal functional overlap of cell envelope lipids in host-pathogen interactions. *Cell Microbiol* **16**: 195–213.
- Perez, E., Samper, S., Bordas, Y., Guilhot, C., Gicquel, B., and Martin, C. (2001) An essential role for *phoP* in *Mycobacterium tuberculosis* virulence. *Mol Microbiol* **41**: 179–187.
- Piddington, D.L., Kashkouli, A., and Buchmeier, N.A. (2000) Growth of *Mycobacterium tuberculosis* in a defined medium is very restricted by acid pH and Mg²⁺ levels. *Infect Immun* **68**: 4518–4522.
- Purdy, G.E., Niederweis, M., and Russell, D.G. (2009) Decreased outer membrane permeability protects mycobacteria from killing by ubiquitin-derived peptides. *Mol Microbiol* **73**: 844–857.
- Rohde, K.H., Abramovitch, R.B., and Russell, D.G. (2007) *Mycobacterium tuberculosis* invasion of macrophages: linking bacterial gene expression to environmental cues. *Cell Host Microbe* **2**: 352–364.
- Rohde, K.H., Veiga, D.F., Caldwell, S., Balazsi, G., and Russell, D.G. (2012) Linking the transcriptional profiles and the physiological states of *Mycobacterium tuberculosis* during an extended intracellular infection. *PLoS Pathog* **8**: e1002769.
- Russell, D.G., Cardona, P.J., Kim, M.J., Allain, S., and Altare, F. (2009) Foamy macrophages and the progression of the human tuberculosis granuloma. *Nat Immunol* **10**: 943–948.
- Sauer, U., and Eikmanns, B.J. (2005) The PEP-pyruvate-oxaloacetate node as the switch point for carbon flux distribution in bacteria. *FEMS Microbiol Rev* **29**: 765–794.
- Savvi, S., Warner, D.F., Kana, B.D., McKinney, J.D., Mizrahi, V., and Dawes, S.S. (2008) Functional characterization of a vitamin B-12-dependent methylmalonyl pathway in *Mycobacterium tuberculosis*: implications for propionate metabolism during growth on fatty acids. *J Bacteriol* **190**: 3886–3895.
- Schneider, C.A., Rasband, W.S., and Eliceiri, K.W. (2012) NIH Image to ImageJ: 25 years of image analysis. *Nat Methods* **9**: 671–675.
- Shi, L., Sohaskey, C.D., Pfeiffer, C., Datta, P., Parks, M., McFadden, J., et al. (2010) Carbon flux rerouting during *Mycobacterium tuberculosis* growth arrest. *Mol Microbiol* **78**: 1199–1215.
- Singh, A., Crossman, D.K., Mai, D., Guidry, L., Voskuil, M.I., Renfrow, M.B., and Steyn, A.J.C. (2009) *Mycobacterium tuberculosis* WhiB3 maintains redox homeostasis by regulating virulence lipid anabolism to modulate macrophage response. *PLoS Pathog* **5**: e1000545.
- Sirakova, T.D., Thirumala, A.K., Dubey, V.S., Sprecher, H., and Kolattukudy, P.E. (2001) The *Mycobacterium tuberculosis* *pks2* gene encodes the synthase for the hepta- and octamethyl-branched fatty acids required for sulfolipid synthesis. *J Biol Chem* **276**: 16833–16839.
- Tan, S., Sukumar, N., Abramovitch, R.B., Parish, T., and Russell, D.G. (2013) *Mycobacterium tuberculosis* responds to chloride and pH as synergistic cues to the immune status of its host cell. *PLoS Pathog* **9**: e1003282.
- Tian, J., Bryk, R., Itoh, M., Suematsu, M., and Nathan, C. (2005) Variant tricarboxylic acid cycle in *Mycobacterium tuberculosis*: identification of alpha-ketoglutarate decarboxylase. *Proc Natl Acad Sci USA* **102**: 10670–10675.
- Timm, J., Post, F.A., Bekker, L.G., Walther, G.B., Wainwright, H.C., Manganelli, R., et al. (2003) Differential expression of iron-, carbon-, and oxygen-responsive mycobacterial genes in the lungs of chronically infected mice and tuberculosis patients. *Proc Natl Acad Sci USA* **100**: 14321–14326.
- Upton, A.M., and McKinney, J.D. (2007) Role of the methylcitrate cycle in propionate metabolism and detoxification in *Mycobacterium smegmatis*. *Microbiology* **153**: 3973–3982.
- Van der Geize, R., Yam, K., Heuser, T., Wilbrink, M.H., Hara, H., Anderton, M.C., et al. (2007) A gene cluster encoding cholesterol catabolism in a soil actinomycete provides insight into *Mycobacterium tuberculosis* survival in macrophages. *Proc Natl Acad Sci USA* **104**: 1947–1952.
- Vandal, O.H., Pierini, L.M., Schnappinger, D., Nathan, C.F., and Ehrt, S. (2008) A membrane protein preserves intracellular pH in intraphagosomal *Mycobacterium tuberculosis*. *Nat Med* **14**: 849–854.
- Vandal, O.H., Nathan, C.F., and Ehrt, S. (2009a) Acid resistance in *Mycobacterium tuberculosis*. *J Bacteriol* **191**: 4714–4721.
- Vandal, O.H., Roberts, J.A., Odaira, T., Schnappinger, D., Nathan, C.F., and Ehrt, S. (2009b) Acid-susceptible mutants of *Mycobacterium tuberculosis* share hypersusceptibility to cell wall and oxidative stress and to the host environment. *J Bacteriol* **191**: 625–631.
- Vilchez, C., Weisbrod, T.R., Chen, B., Kremer, L., Hazbon, M.H., Wang, F., et al. (2005) Altered NADH/NAD⁺ ratio mediates coresistance to isoniazid and ethionamide in mycobacteria. *Antimicrob Agents Chemother* **49**: 708–720.
- Vilchez, C., Av-Gay, Y., Attarian, R., Liu, Z., Hazbon, M.H., Colangeli, R., et al. (2008) Mycothiol biosynthesis is essential for ethionamide susceptibility in *Mycobacterium tuberculosis*. *Mol Microbiol* **69**: 1316–1329.
- Walters, S.B., Dubnau, E., Kolesnikova, I., Laval, F., Daffe, M., and Smith, I. (2006) The *Mycobacterium tuberculosis* PhoPR two-component system regulates genes essential for virulence and complex lipid biosynthesis. *Mol Microbiol* **60**: 312–330.

Supporting information

Additional supporting information may be found in the online version of this article at the publisher's web-site.